Mixed Halide Perovskite Solar Cell with Activated Carbon as Hole Transporting Material

S. Raju [a, b], R. Gupta [a, b] A.K.Arof [b*,] Ranu Nayak [a*]

[a-] *Amity Institute of Nanotechnology, Amity University, Noida, U.P., India, 201301*

[b-] *Centre for Ionics University of Malaya, Department of Physics, Faculty of Science, University of Malaya, Kuala Lumpur, Malaysia 50603*

Abstract

In this study, Activated carbon along with PEMA as plasticizer is investigated as a replacement for Spiro-OMeTAD. The basic structure of the fabricated solar cell was: FTO/compact layer/mesoporous TiO_2/$CH_3NH_3I_{3-x}PbCl_x$/Activated carbon-PEMA. The perovskite and the activated carbon slurry are both prepared using simple solution processing method. The FESEM analysis of the perovskite film shows the formation of large crystallites. XRD analysis further confirms the crystalline structure. The lattice planes of (110), (210), (220), and (310) at 2θ angles12.64°, 14.09°, 28.5°, and 31.83° respectively reviews that the crystalline perovskite is in Tetragonal phase. UV-Vis absorption spectrum of the activated carbon coated perovskite cell shows high absorption covering UV and visible region of the electromagnetic spectrum. A large bandgap of 1.65eV was obtained for perovskite film. Various compositions of the activated carbon has been investigated in which the 20% activated carbon shows the best performance. The 20% activated Carbon shows an open circuit Voltage of **0.42**V with current density of **11.35**mA cm^{-2}. The corresponding photo conversion efficiency is **1.2**% with a Fill Factor of **31**%.

Keywords: perovskite solar cell, $CH_3NH_3I_{3-x}PbCl_x$ perovskite, Activated Carbon.

I *Introduction*

Perovskite Solar Cells are the present trend in solar cell technology because of their incredibly high efficiency comparable with that of silicon solar cells. The conventional perovskite based solar cells developed use Spiro-OMeTAD as the hole-transport material. Besides Spiro-OMeTAD the Activated carbon is chosen as hole-transport material because to extract and harness more of the incoming solar radiation. Activated carbon not only has similar optical band gap as that of spiro-OMeTAD but also has matching valence band maximums. The optical bandgap of activated carbon is 3.18eV, whereas that of spiro-OMeTAD is 2eV. The valance band maximum of activated carbon is about -5.1eV and that of spiro-OMeTAD varies between -5.21eV to -5.30eV. Activated carbon has wider range of absorption in UV- region than Spiro OMeTAD along with the additives i.e., bis (trifluro-methane) sulfonimide lithium salt (LiTFSI) and 4-*tert*-butylpyridine (tBP).

II *Experimental*

Materials: Diisopropoxytitanium bis(acetylacetonate) solution, titanium (IV) chloride Solution, were purchased from Aldrich, Lead Chloride (98%), poly(ethyl methacrylate), was purchased from Sigma-Aldrich, Methylammonium iodide from Solaronix, Nanoporous Titanium (II) oxide was purchased from Dye-Sol (Sun 2), Activated Carbon from Kurary Chemical, Dimethylformamide (DMF), Nitric Acid, was purchased from Friendemann Schmidt, Toluene was purchased from Mallinckrodt chemicals, Hydrochloric acid(36%) was purchased from Ajax Chemicals, Ethanol(95%) was from John. Kollin chemicals and Zinc (metal) Powder was from Systerm.

Synthesis of Methylammonium Lead mixed halide Perovskite: In the typical experiment Lead Chloride and Methylammonium iodide were made to react in an organic medium. Dimethylformamide shortly denoted as DMF was used as a solvent media. The

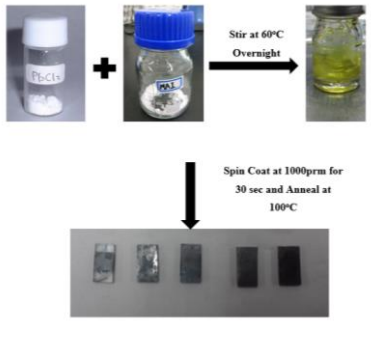

a

Sl no	Weight percentage of activated carbon (%)	Activated Carbon weight (g)	PEMA (g)	Toluene (ml)
1	90	0.09	0.01	1
2	80	0.08	0.02	1
3	70	0.07	0.03	1
4	60	0.06	0.04	1
5	50	0.05	0.05	1
6	40	0.04	0.06	1
7	30	0.03	0.07	1
8	20	0.02	0.08	1
9	10	0.01	0.09	1

b

c

d

Fig 1: a) Actual Synthesis Process. b) Table: composition of the activated carbon slurry. c) The prepared activated carbon coatings. d) The prepared devices

composition of the precursor was restricted to 40% wt. and the weight ratios of MAI to lead chloride was maintained to 3:1. The precursor solution was allowed to react for 24 hrs maintaining a temperature of 80°C.

Preparation of activated carbon slurry: Activated carbon slurry was prepared in Toluene with PEMA as plasticizer. A weight percentage composition was followed for the slurry preparation. The table 1b gives the compositional values of the slurry. The solution mixture was stirred for 48 hours at 80°C. A smooth slurry was obtained. This was spin coated onto the perovskite coated substrates at 3000 rpm for 50 secs. Later the coated substrates were annealed at 80°C for 45 mins.

Fabrication of Perovskite solar cell: The main elements of the device are the $CH_3NH_3I_{3-x}PbCl_x$ perovskite layer and the Activated carbon (Hole-transport) layer. The perovskite solar cell are prepared on a FTO glass substrate with dimension 1x2.5cm^2. The substrates were etched at 1/3rd of the full length to provide Anode contact. Then after washing and cleaning a blocking layer of Titanium diisopropoxide bis-acetyleneacetone in ethanol was coated. After the blocking layer was coated 18nm Nanoporous TiO_2 was coated which upon annealing became 30nm in size. After the Nanoporous TiO_2 coating the substrates were treated with $TiCl_4$ for the increased stability. Later the prepared perovskite was spin coated at 1000 rpm and annealed at 100°C. Then the activated carbon was coated onto the perovskite layer and annealed to evaporate the solvent. To make the device complete, counter electrodes were prepared using gold. Gold was sputtered on to the coated activated carbon layer. A 100nm gold layer was sputtered using the sputtering device. The Prepared devices are as shown in the fig 1d.

III *Results and Discussion*

Microscopic Analysis: Microscopic images of the prepared perovskite layer is obtained and is as shown in fig 2a. It can be observed from the figures that there are many number of small crystals. We could exactly say that the formed structures are because the structures formed are shining and it ould also be observed that the light transmitted through the structures. This was the first confirmation about the formation of the crystals. About 98% of the surface is being covered. This infers that the pin hoes are very less. For further confirmation of the exact morphology FESEM analysis was done.

FESEM Analysis: FESEM- Field Emission Scanning Electron Microscopy was carried out for the surface morphology studies. All the FESEM Analysis is done on SU8200 from Hitachi at 2kV. The same is elucidated in fig 2b, 2c, 2d. It can be clearly seen from fig 2b that a uniform film is formed which is

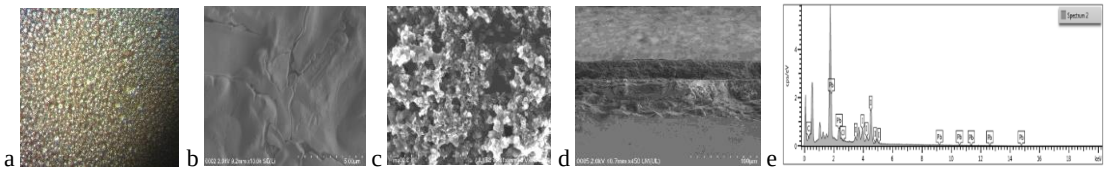

Fig 2: a) Microscopic Image of the prepared Perovskite film b) FESEM images of the $CH_3NH_3I_{3-x}PbCl_x$ perovskite film. c) FESEM image of the 20% activated carbon layer d) cross sectional image of the device e) EDX of the Perovskite Film

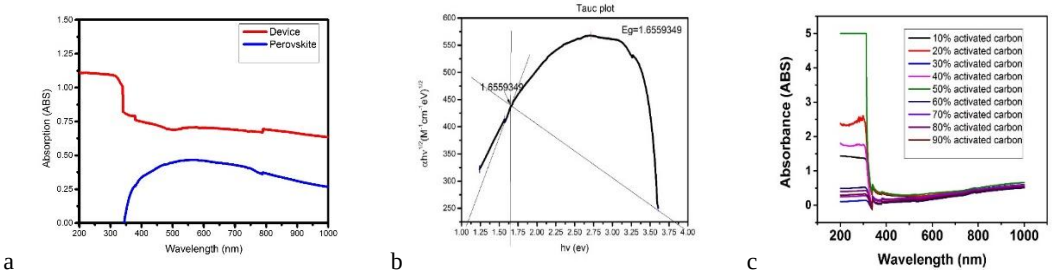

Fig 3: a) UV-Vis Absorption Spectrum of the Perovskite Film. b) Tauc Plot of the perovskite film. c) UV-Vis Absorption Spectrum of Activated Carbon Coated Samples without perovskite.

taken at 50µm. Also from the other images it is clearly seen that micron sized gains are formed. This indicates that large sized crystals are formed. For the elemental conformation EDX was taken. Fig 2e shows the EDX plot for the sample chosen. Fig shows the activated carbon thin film images. Fig 2d shows the complete device layers.

UV-Vis Analysis: The Absorption spectrum of the perovskite shows a wide absorption from 350nm to 800nm. Fig3a is the UV-Vis absorption of the Perovskite and the device. The Absorption peak is shown at 748nm for the perovskite film. The device shows a complete absorption in the UV-Visible region of the electromagnetic spectrum. Fig 3b shows the Tauc Plot also known as the Kubulk Munk Plot. The Tauc Plot is used for the calculation of the optical bandgap of the material. The first peak in the Tauc Plot is taken for the calculation of the optical band gap E_g. The energy corresponding to the wavelength is calculated using the formula

$$hv = \frac{1240}{\lambda}$$

Where h= Planck's constant, v= frequency and λ = wavelength (nm). The absorption coefficient were calculated from the formula

$$\alpha = \frac{2.303A}{\tau}$$

Where α =absorption coefficient, A= Absorbance of the material and τ= thickness of the material

A graph of $\boldsymbol{\alpha h v^{1/2}}$ versus $\boldsymbol{hv}$ is plotted which is called the Tauc plot. The value ½ indicates the direct transition of the electrons from one layer to the other within the device. From the Tauc Plot it was observed that the optical bandgap of the perovskite is found to be 1.656eV. This is a large value as compared to the previously reported. The Absorption spectrum of the activated carbon is shown is fig 3c. It can be observed that the ratio of activated carbon to PEMA greatly affects the absorbance of the activated carbon. All the samples showed strong and prominent absorption between 200nm to 300nm which is in the UV region of the electromagnetic spectrum. As the quantity of the activated carbon increased the absorbance of the light also increased till 50 percent of the activated carbon. Later on the higher proportionate of activated carbon showed comparatively lesser absorption of light. 50 percent sample showed the highest absorbance of UV light.

X-Ray Diffraction Analysis: The crystallinity of the perovskite film formed is enumerated from the X-Ray Diffraction

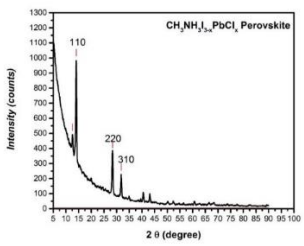

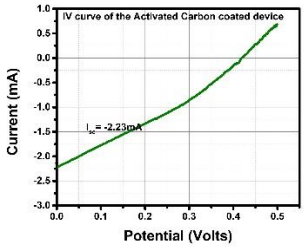

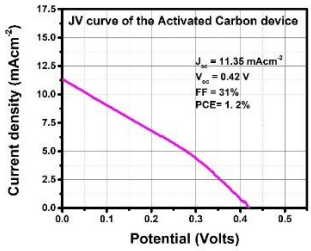

	Jsc (mA cm^{-2})	Voc (Volts)	FF	PCE (%)	Area (cm^2)
20%	11.35	0.42	0.31	1.24	0.196
50%	3.22459	0.0818	0.22313	0.005885	1.15
60%	3.0331	0.06732	0.21348	0.00435	1.045
70%	1.136781	0.02204	0.032825	0.000822	1

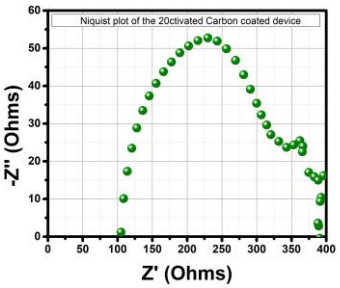

Fig 4: a) XRD plot of the $CH_3NH_3I_{3-x}PbCl_x$ perovskite flim b) IV characteristics of the 20% activated carbon coated device c) JV plot of the 20% activated carbon device d) table showing the PCE values for the various activated carbon coated devices e) Niquist plot of the 20% Activated Carbon device.

patterns. High degree of crystallinity is observed for the perovskite precursors as well as the Perovskite film itself. Sharp peaks in the patterns indicate the crystalline nature of the perovskite film. It is also observed almost pure crystalline phase of the perovskites are formed because of the lesser impurity peaks. Planes were found at 110, 220 and 310 at a 2θ values of 14.093°, 28.497°, 31.825° respectively. This is seen in fig 4a. Fig, and shows the powder XRD patterns of $PbCl_2$ and MAI. Planes were found at 15.0757°, 23.3410°, 30.6565°, 36.6337° which corresponded to planes 110, 200, 220, 221 in $PbCl_2$ and in MAI, planes were found at 19.856°, 30.051°, 44.052°, 51.58° corresponding to 110, 200, 300, and 220. The hkl values of the XRD pattern of the perovskite film clearly indicates the formation of the perovskite in tetragonal crystal structure. The grain size or the average crystallite size can be related to the incident wavelength and the 2θ for a particular plane using Scherer equation. The Scherer equation is as described below.

$$\tau = \frac{k * \lambda}{\beta * cos\theta}$$

Where τ = average crystallite size, K = shape factor, which is usually near to unity, and depends upon the grain shape. = 0.9 in our case, λ = wavelength of the X-rays = 0.15406nm, β = line width at half the maximum (in radians) and θ = Braggs angle (radians). To calculate the average crystallite grain size of the perovskite thin film, the peak at the plane 110 at 2θ = 14.093° was used. The Calculated average grain size of the prepared perovskite thin film is 107nm.

Photovoltaic measurements: Photovoltaic measurements were done using Metrohm Autolab PGSTAT128N, FRA32M. The device was illuminated under 1 Sun conditions (100 mW cm^{-2} AM1.5G). The area of respective samples and the obtained open circuit Voltage, Current density, Fill factor and the photo conversion efficiency are as tabulated in the table. The respective nature of the current and the resulting current density due the current obtained are as shown in fig and. It is observed that the 20% activated carbon sample showed the maximum yield producing a large output voltage of 0.42V as compared to the other samples. To further confirm the produced voltage, the 20% activated carbon coated

sample was subjected to repeated measurement. There was almost constant production of the open circuit voltage. The corresponding current densities, fill factor and the photo conversion efficiency are as tabulated in table. The IV and JV plots of 20% activated carbon sample are shown in fig and respectively.

Impedance Spectroscopy: A solar power systems is sometimes subject to rapid insolation variation during propagation of clouds. More important is the loading of the photovoltaic system with switched capacitive and inductive loads. Certainly, it is required to study the performance of the system under these transient conditions. The study can be applied equally well to large area photodetectors working under rapid signal variations. To describe the performance of the solar cell as a power device, its I-V characteristic is necessary but not sufficient. It is now required to accurately determine the transit time τ and the series resistance. This will be carried out by measuring the forward impedance as a function of frequency and biasing. The biasing is considered here as a parameter because the transit time may depend on the injection level. The Impedance measurements were done using Metrohm Autolab PGSTAT128N, FRA32M. The devices which were named after their composition of the Activated Carbon. The Open Circuit voltages were obtained from the Photovoltaic Measurements. The same values were used as the biasing voltages for the devices of respective compositions. For 20%Activated carbon coated sample the biasing voltage was 0.42V, for 50% Activated Carbon coated sample, the biasing voltage was 0.0818V. Similarly for 60% and 70% Activated Carbon Coated Sample the biasing voltages were 0.06732V and 0.02204V respectively. The obtained Nyquist and the Bode plots are as shown in the fig and respectively. From the Nyquist plot it can be observed that the value of the AC impedance is much lower as the curve does not increase. The Charging Behavior of the device is not observed as the curve at the end of the cycle is not increasing and rather loops. This is due to the inductive behavior of the device. Assuming that the small signal parameters of the solar cell are independent of frequency and that the dc cell current is small enough that the current crowding effect is small, the terminal impedance diagram takes the form of a circle as shown in Fig.

Conclusion: The work has been done to investigate $CH_3NH_3I_{3-x}PbCl_x$ Perovskite Solar Cell. The UV-Vis Absorption spectrum confirms the absorption of device in the entire UV-Visible region of the electromagnetic spectrum. The Electrical performance of the 20% Activated Carbon shows a maximum open circuit voltage of 0.42V with a current density of 11.35 $mAcm^{-2}$. The corresponding Photo conversion efficiency is 1.2% with a Fill Factor of 31%.

IV *References*

Supplementary Information:

Sample Preparation: All the sample FTO glasses were cleaned ultrasonically in De-Ionized water, Acetone followed by Isopropyl Alcohol for 22 mins. Later the samples were etched using 0.2M HCl and Zinc powder. After etching the samples were cleaned again in detergent, De-Ionized water, and Isopropyl Alcohol in an Ultrasonicator for 15 mins in each solvent. Later the sample FTO's were dried and preserved for later use.

Coating of Blocking Layer: A blocking Layer is required for to avoid any short circuiting that might occur during the final device fabrication. This was achieved using Titanium Diisopropoxide bis-acetylacetone. A coating slurry was prepared by diluting Titanium Diisopropoxide bis-acetylacetone with ethanol in a ratio of 1:10. The sample FTO's were coated with the base layer at 4000rpm for 60 seconds. The base layer coated samples were then sintered at 450ºC for 30 mins, at a ramp rate of 3ºC/min. Later the samples were allowed to cool down to room temperature.

Coating of Nanoporous TiO_2: Dye sol nanoporous TiO_2 was coated as the active electron transporter layer to the cathode of the final device. The size of the nanoporous TiO_2 was 18nm. For the coating solution the Dye Sol TiO_2 was diluted in ethanol in a 1:3 for Dye: ethanol. This was coated on the base layer coated sample FTO's at a spin speed of 4000rpm for 30 seconds. Later the samples were sintered at 450ºC for 30 mins at a ramp rate of 3ºC/min. After this the samples were allowed to cool down to room temperature for later use.

$TiCl_4$ Treatment: The nanoporous TiO_2 coated samples were treated with $TiCl_4$ for the stabilization of the Nanoporous TiO_2 coated on the samples. During this treatment the size of the nanoporous TiO_2 increased to 30nm. This was achieved by using 4mM $TiCl_4$. For the preparation of $TiCl_4$ 400ml DI water was kept in bath until the temperature of DI water reached 2ºC. When the temperature was attained 1ml $TiCl_4$ was injected into the frozen DI water. Then the solution was then stirred until the temperature reached 70ºC. At this the nanoporous coated TiO_2 were immersed in the $TiCl_4$ solution. The samples were kept for exactly 30mins and later they were removed and wiped using wipes. The wiped samples were then sintered at 500ºC for 30 mins at a ramp rate of 3ºC/min. When the sintering was complete the samples were allowed to cool to room temperature and preserved.

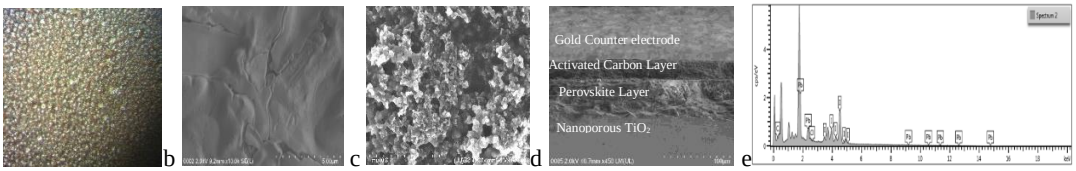

Fig 2: a) Microscopic Image of the prepared Perovskite film b) FESEM images of the $CH_3NH_3I_{3-x}PbCl_x$ perovskite film. c) FESEM image of the 20% activated carbon layer d) cross sectional image of the device e) EDX of the Perovskite Film

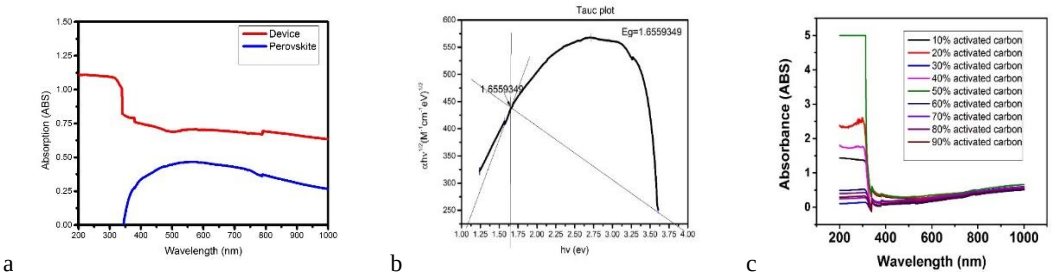

Fig 3: a) UV-Vis Absorption Spectrum of the Perovskite Film. b) Tauc Plot of the perovskite film. c) UV-Vis Absorption Spectrum of Activated Carbon Coated Samples without perovskite.

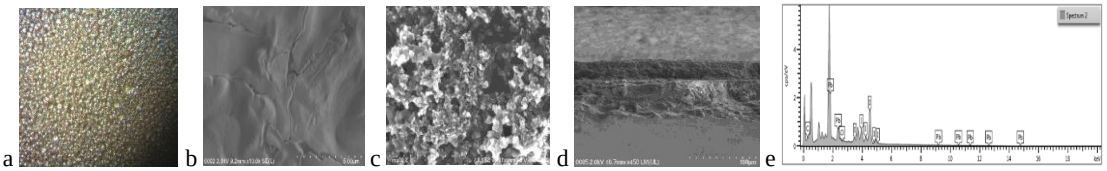

Fig 2: a) Microscopic Image of the prepared Perovskite film b) FESEM images of the $CH_3NH_3I_{3-x}PbCl_x$ perovskite film. c) FESEM image of the 20% activated carbon layer d) cross sectional image of the device e) EDX of the Perovskite Film

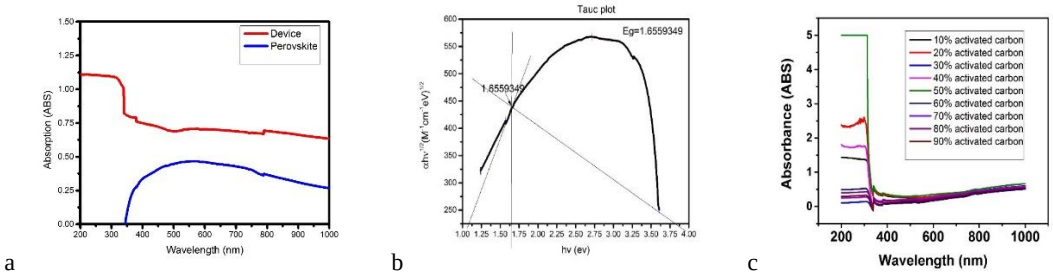

a b c

Fig 3: a) UV-Vis Absorption Spectrum of the Perovskite Film. b) Tauc Plot of the perovskite film. c) UV-Vis Absorption Spectrum of Activated Carbon Coated Samples without perovskite.

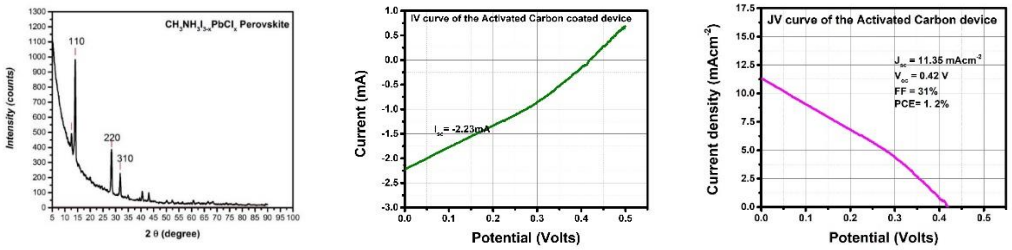

	Jsc (mA cm^{-2})	Voc (Volts)	FF	PCE (%)	Area (cm^2)
20%	11.35	0.42	0.31	1.24	0.196
50%	3.22459	0.0818	0.22313	0.005885	1.15
60%	3.0331	0.06732	0.21348	0.00435	1.045
70%	1.136781	0.02204	0.032825	0.000822	1

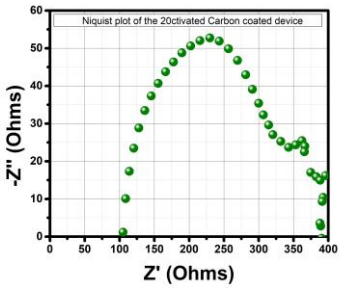

Fig 4: a) XRD plot of the $CH_3NH_3I_{3-x}PbCl_x$ perovskite flim b) IV characteristics of the 20% activated carbon coated device c) JV plot of the 20% activated carbon device d) table showing the PCE values for the various activated carbon coated devices e) Niquist plot of the 20% Activated Carbon device.

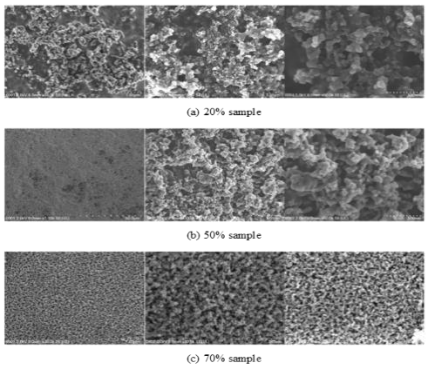

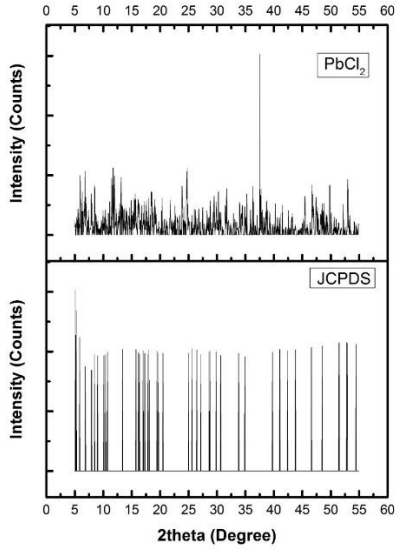

Fig: XRD pattern of the $PbCl_2$

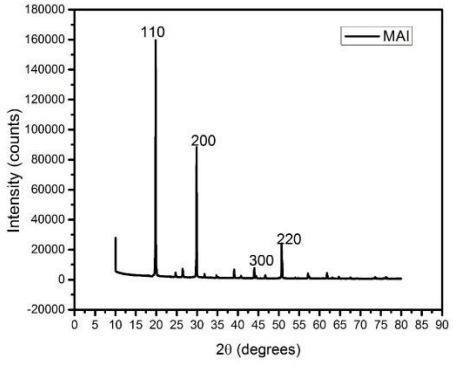

Fig: XRD pattern of Methylammonium Iodide

Table: The electrical parameters obtained for different percentage compositions of the activated carbon.

	Jsc (mA cm^{-2})	**Voc (Volts)**	**FF**	**PCE (%)**	**Area (cm^2)**
20%	11.35	0.42	0.31	1.24	0.196
50%	3.22459	0.0818	0.22313	0.005885	1.15
60%	3.0331	0.06732	0.21348	0.00435	1.045
70%	1.136781	0.02204	0.032825	0.000822	1

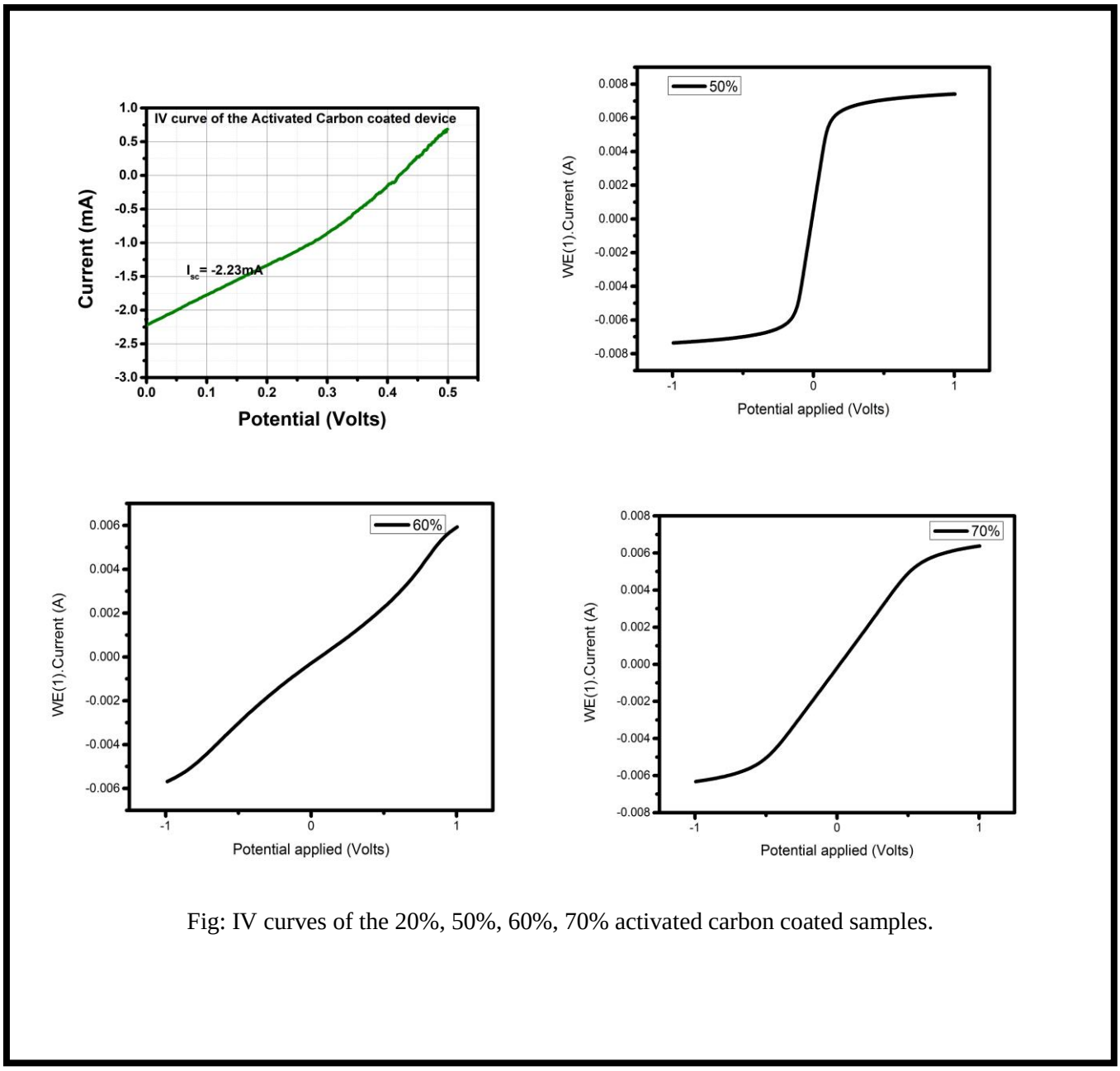

Fig: IV curves of the 20%, 50%, 60%, 70% activated carbon coated samples.

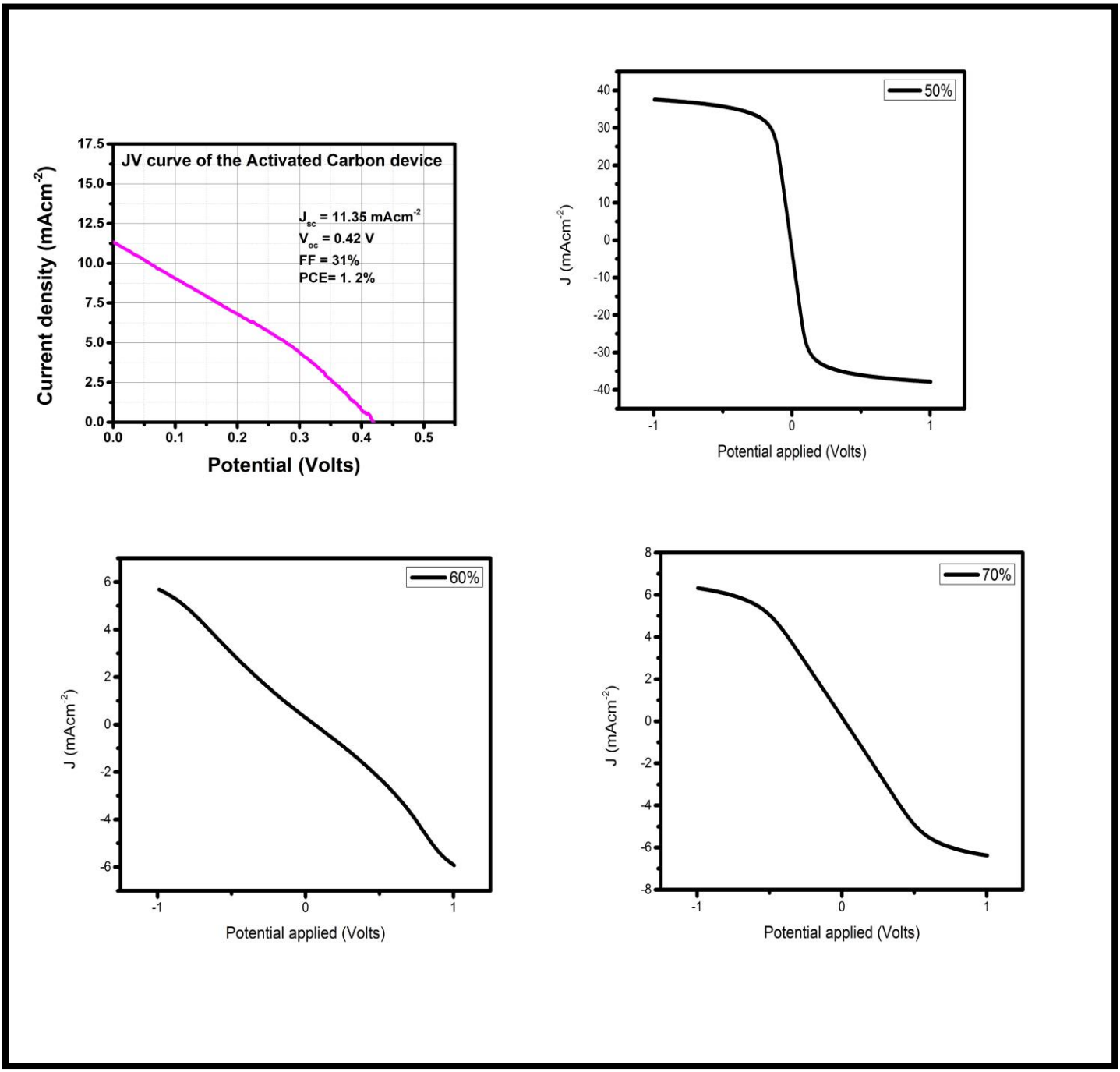

Fig: JV curves of 20%, 50%, 60% and 70% respectively

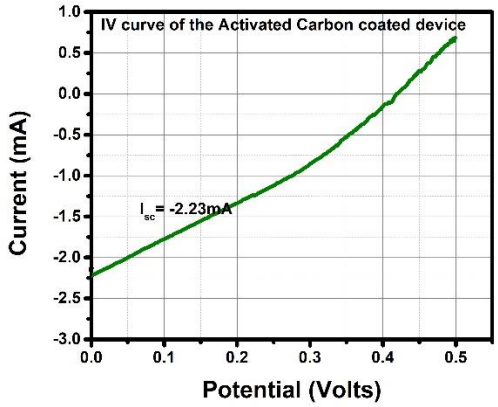

Fig: IV characteristics of 20% Activated Carbon Coated sample.

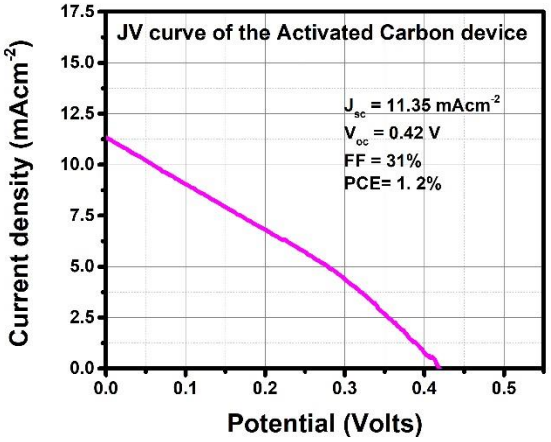

Fig: JV curves of 20 % activated carbon coated samples for various runs

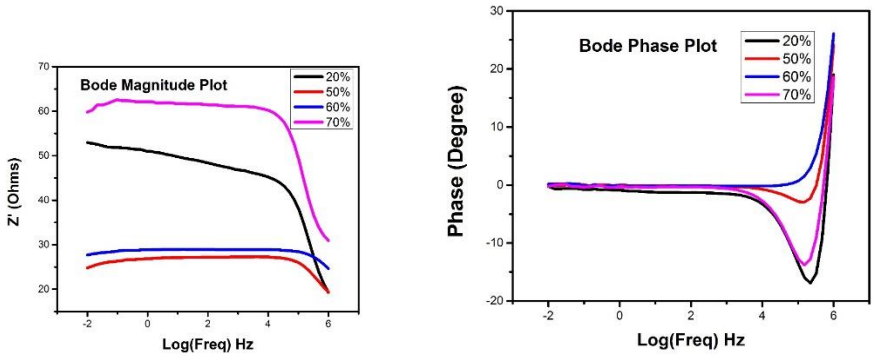

Fig: Bode Magnitude and Phase plots for different composition of the activated carbon.

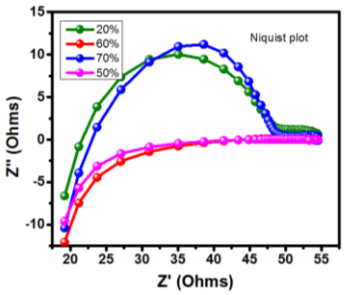

	Jsc (mA cm^{-2})	Voc (Volts)	FF	PCE (%)	Area (cm^2)
20%	11.35	0.42	0.31	1.24	0.196
50%	3.22459	0.0818	0.22313	0.005885	1.15
60%	3.0331	0.06732	0.21348	0.00435	1.045
70%	1.136781	0.02204	0.032825	0.000822	1

Fig: Nyquist plot for the different compositions of the activated carbon coated samples